Journal of Crystal Growth 35 (1976) 15–28

GROWTH ON IMPERFECT CRYSTAL FACES
I. Monte-Carlo growth rates

G.H. GILMER
Bell Laboratories, Murray Hill, New Jersey 07974, USA

Received 1 April 1976; revised manuscript received 5 May 1976

The contribution of screw dislocations to the growth of low index faces is assessed by means of a simple analytical model and the Monte-Carlo method. The (001) face of a simple cubic lattice gas is employed in the numerical calculations. Growth rates of a perfect crystal are compared with those of a similar model which contains a pair of screw dislocations. The data cover a wide range of temperatures and driving forces. Surface mobility is included in one case, and the increase in the growth rate is compared with that predicted by an analytical model of the surface migration of adatoms.

1. Introduction

The growth rate of a cyrstal is related to a number of factors which determine the condition of the crystal–fluid interface. Among these are the atomic bonding in the surface layer, the mobility of the atoms at the surface, the degree of perfection of the growing crystal, surface roughness, and impurities. It is difficult to achieve the control necessary to isolate and examine each of these factors in the laboratory. The presence of small quantities of impurities in the bulk of the system may have a major effect on the kinetics. Also, factors such as adatom mobility cannot be altered without changing the temperature and hence the interface roughness and the driving force.

Computer simulation models are ideally suited for such a study, since each parameter can be varied independently. For example, the activation energy for adatom diffusion can be changed without affecting the bond strength or the temperature. In recent years computer simulations have been used to study various aspects of crystal growth including the surface roughening transition [1–4], the equilibrium structure and kinetics of steps on low index surfaces [5–7], and epitaxy [8].

The importance of dislocations in crystal growth was first pointed out by Frank [9] who realized that they could enhance the growth rate of low index faces by many orders of magnitude. A dislocation that terminates with a component of its Burger's vector perpendicular to the surface circumvents the difficult process of nucleating new layers. The step which terminates on this dislocation can wind up into a steady-state spiral, and thereby provide a continuous source of edge positions. Two-dimensional (2-D) nucleation is unnecessary. Dislocations are especially important at low temperatures and driving forces, where the growth rate of a perfect crystal face is essentially zero.

But many aspects of the spiral growth process have not been investigated. Vapor deposition experiments are usually performed in the presence of a large driving force, and 2-D nucleation can proceed at an appreciable rate. The importance of dislocations is open to question in this case. Also, the relation between dislocations and the formation of hillocks on vapor-grown crystals requires consideration.

At a temperature close to the melting point, the surface atoms of a crystal in equilibrium with its vapor may become disordered, since they have fewer bonds to the crystal than atoms in the bulk. Most of the faces are predicted to experience a roughening transition at a temperature T_R below the melting point [10,11]. At this temperature the edge free energy of a step becomes zero. The formation of new layers on a perfect crystal surface

may occur readily even at low driving forces. It is well established from the work of Jackson [11,12] that crystals with a low entropy of fusion grow from the melt without facets. This apparently means that all of the faces are thermally rough, and it is not expected that dislocations would affect the kinetics. But spiral growth models have been invoked to explain the growth kinetics in these systems. In fact, the influence of dislocations on the growth of rough surfaces has not previously been investigated, and it is important to evaluate quantitatively the effect of dislocations on the growth rate for various temperatures, driving forces, and adatom mobilities.

Section 2 contains a description of the model employed and the simulation techniques. Section 3 presents a simple analytical model of growth applicable to large driving forces where new layers may be readily nucleated, but where dislocations are also present. In addition, the range of temperature and driving force where dislocations play a dominant role in the growth kinetics is described. Section 4 contains a comparison of the Monte-Carlo growth rates of crystals with dislocations to those of perfect crystals.

In a subsequent paper we investigate the surface structure resulting from steady-state growth on a surface intersected by a dislocation; growth rates of vicinal faces are measured and related to the formation of hillocks at the dislocations.

2. The model

We use the solid-on-solid (SOS) model of a simple cubic (001) face in all of the computations. This is a generalization of the familiar terrace–ledge–kink model [10] in the sense that it permits clusters of adatoms, surface vacancies and irregular step structures. But it is a special case of the lattice gas model since it is required that each atom have another one directly below it, i.e., overhangs are excluded. In the low temperature range investigated here the SOS model is an accurate approximation to the lattice gas, because the surface remains quite flat and overhangs are energetically unfavorable. The surface configuration is represented by a rectangular array of integers which specifies the number of atoms in each column perpendicular to the (001) plane.

The atomic kinetics are nearly identical to those employed in most previous studies of this model. Atoms impinge at random positions on the surface and at an average rate of k^+ per site. Surface atoms evaporate at a rate

$$k_n^- = \nu \exp(-n\varphi/kT) , \tag{1}$$

where ν is a frequency factor and n is the number of nearest neighbors. The energy φ is required to break the bond with one neighbor, k is Boltzmann's constant, and T the temperature. The impingement rate is proportional to the pressure in a pure vapor system, and in general we write

$$k^+ = \exp(\Delta\mu/kT)\, k_3^- , \tag{2}$$

where $\Delta\mu$ is the deviation of the chemical potential at the interface from the crystal–fluid equilibrium value. With $\Delta\mu = 0$, $k^+ = k_3^-$ and the impingement rate is equal to the kink site evaporation rate, as required.

In the case of surface migration, some flexibility is allowed in the choice of transition probabilities. In this work, a surface atom with n neighbors jumps to a site where it would have m neighbors at the rate

$$k_{nm} = \tfrac{1}{8}\nu \exp\{-[E_{sd}(n,m) + \Delta E(n,m)]/kT\}. \tag{3}$$

We choose $E_{sd}(n,m) \equiv E_{sd}(m,n)$ as the activation energy for a jump to a site where $m \geqslant n$, and this parameter determines the mobility of the adatoms. The parameter $\Delta E(n,m)$ is chosen to be positive only if the number of neighbors at the second site is less than that of the first, and zero otherwise:

$$\Delta E(n,m) = \begin{cases} (n-m)\varphi & \text{if } m \leqslant n, \\ 0 & \text{if } m > n . \end{cases} \tag{4}$$

Microscopic reversibility is satisfied by this choice since $k_{nm}/k_{mn} = \exp\{(n-m)\varphi/kT\}$ in all cases. This choice of surface diffusion rates implies that an adatom ($n = 1$) near a step has the same probability of jumping to a neighboring site in the edge of a step ($m = 2$–4) as it has of jumping to another site with no lateral neighbors. Since small lattice distortions and long-range forces are excluded, it seems appropriate to choose k_{nm} to satisfy this condition. Note that k_{nm} depends only on n and m, and is not changed when the two sites are at different levels. Two adatoms on either side of a step have equal probabilities of jumping into the edge of the step, for example, even though one must change levels in order to make the jump. This excludes the possibility of step bunching as a result of asymmetric capture at the step [14].

The values of $E_{sd}(n,m)$ employed in these calculations are chosen to yield a large adatom mobility, and yet retain a simulation algorithm which does not consume excessive amounts of computer time. Specifically,

$$E_{sd}(n,m) = \begin{cases} \varphi/2, & \text{if either } m = 1 \text{ or } n = 1, \\ 3\varphi/2, & \text{if } n \text{ and } m > 1, \text{ and either } m = 2 \text{ or } n = 2, \\ 5\varphi/2, & \text{if } n \text{ and } m > 2. \end{cases} \quad (5)$$

According to (3), (4), (5) and (1), a surface diffusion jump to a site with $m \geqslant n$ occurs more frequently than evaporation, as would be expected in reality. Surface migration permits atoms which impinge on sites of high energy to move to lower energy positions where the evaporation rate is lower.

There is a practical reason for choosing $E_{sd}(n,m)$ larger for larger values of n and m. Clearly most of the computer time required to process the simulation is involved in performing the surface migrations of atoms which have a high jump probability. But at low temperatures the number of one and two-bonded atoms is small, and hence the number of sites which require most of the computer time is small.

To take advantage of this situation, it is necessary to know where the atoms with high jump probabilities are located, and to select these sites more frequently than the others [16]. The Monte-Carlo algorithm maintains a list of the surface atoms in the order of their coordination. The cycle begins by selecting a subset of the surface atoms which includes all N_n atoms with n bonds. This subset is chosen with a probability

$$p_n = N_n(k_n^- + k^+ + k_{nn}) / \sum_{i=1}^{5} N_i(k_i^- + k^+ + k_{ii}) .$$

Then a surface atom is chosen at random from this list; and finally the option of impingement, evaporation, or surface migration is chosen with probabilities proportional to k^+, k_i^-, and k_{ii}, respectively. If surface migration is chosen, one of eight lateral neighboring sites is selected and the jump is executed with a probability of k_{ij}/k_{ii}, where j is the coordination of the selected site. (Direct jumps to the four nearest, and the four next nearest neigbor sites are permitted.)

The computer time required to add a certain number of atoms to the crystal is more or less proportional to

$$k^+ / \sum_i N_i(k_i^- + k^+ + k_{ii}) ,$$

the ratio of the probability for impingement to the sum of all the probabilities. The denominator is largely determined by the k_{ii} terms, since in general $k_{ii} > k_i^-$ and $k_{ii} > k^+$. The efficiency of the computation is greatly enhanced if one chooses k_{ii} to be small for large i where N_i is also large, and for this reason the activation energy $E_{sd}(n,m)$ in eq. (5) is chosen to be high for the larger values of m and n.

Various array sizes up to 100 X 100 sites are utilized in the computations, and in no case is a size dependence observed. Periodic boundary conditions are applied at the edge of the array. A pair of opposite screw dislocations is simulated through a modification of atomic bonds which cross a rectangular segment of a (010) plane, as shown in fig. 1. The rectangle ABCD is bounded by the dislocation lines AB and CD, and by the two (001) surfaces of the crystal. Atoms immediately to the left of the rectangle form bonds to atoms on the right in the layer b units higher. Here b is the magnitude of the Burgers vector of the dislocation pair in units of the layer spacing. This is equivalent to displacing the lattice, but it is simpler to program [17]. Strain energy along the dislocation line is not considered in these calculations, although this can be an important factor during the etching of crystal surfaces [18].

Note that the atoms in the row to the left of the line AD are in positions equivalent to the edge of a step, since there are no atoms on the right in the level

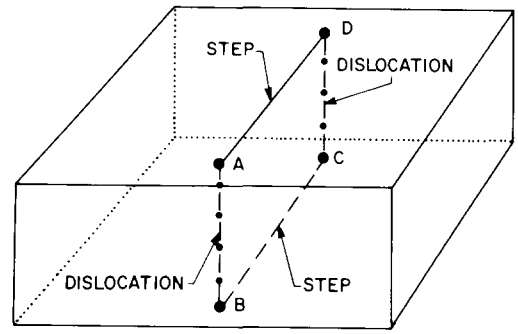

Fig. 1. Diagram illustrating the geometry of the screw dislocations. Interactions crossing plane ABCD are displaced vertically by an amount equal to the Burger's vector of dislocations AB and CD.

above. This "step segment" bows out into a loop and generates new layers by a mechanism equivalent to the Frank–Reid source for dislocation multiplication.

3. Spiral growth and concomitant 2-D nucleation

The effect of screw dislocations on crystal growth is directly related to the edge free energy of steps on the surface. At low temperatures the nucleation of 2-D clusters is improbable at low driving forces because of the high free energy required to form the closed step surrounding the cluster. The atoms at the edge of the cluster are in positions similar to those in the edge of a step, and at low temperatures these have an extra free energy which is approximately equal to the energy of the missing lateral bonds. The rate of 2-D nucleation is extremely small and a source of steps such as that afforded by the dislocations causes a drastic increase in the rate of growth.

On the other hand, near the roughening temperature T_R the step free energy is very small [5]. Even in equilibrium large clusters may form since the restraining influence of the step free energy is small. With only a minute driving force many of these clusters are already larger than the critical size for a 2-D nucleus, and even the perfect crystal grows quite readily. Dislocations are not expected to have a significant effect on the growth rate.

The influence of dislocations is also affected by the magnitude of the driving force. At high driving force where atoms impinge on a site at a rate approaching the evaporation rate of adatoms, 2-D clusters are numerous and nucleation is very fast. Again the dislocations are not expected to have a large effect.

The striking dependence of the growth kinetics on temperature may be seen in fig. 2. Here we have a plot of Monte-Carlo growth rates on the (001) face of a perfect crystal. The numbers adjacent to the curves indicate the ratio L/kT, where $L = 3\varphi$ is the binding energy of the simple cubic crystal. The surface roughening temperature occurs at $L/kT_R \cong 4.9$ [11], and hence only the $L/kT = 4.5$ data represent growth above the roughening point. The finite slope of this curve near the origin demonstrates that the nucleation of new layers is not a rate-limiting process. At $L/kT = 6$, a very small nucleation barrier is present, and at even lower temperatures the growth rate is essentially zero

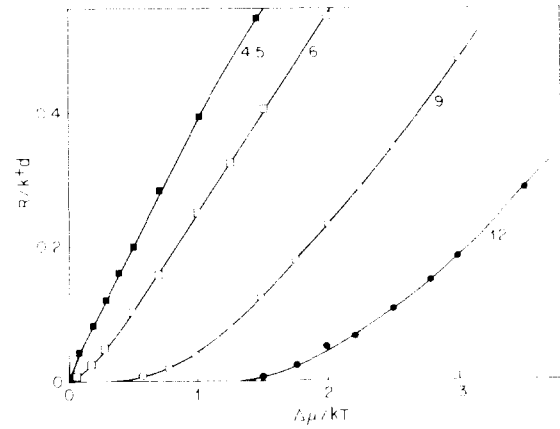

Fig. 2. Normalized growth rates of perfect crystal (001) faces plotted as a function of $\Delta\mu/kT$ for several different values of L/kT.

over a large range of $\Delta\mu$. It is evident that screw dislocations cause the largest changes in the kinetics in the range of $\Delta\mu$ where the growth rate of the perfect crystal is small.

In order to make these concepts more precise, we consider the theory of spiral growth in the presence of 2-D nucleation. The rate of 2-D nucleation is determined by the distribution of clusters on the surface. In the absence of nucleation, the probability of finding a cluster of n atoms on a particular site is [19, 20]

$$p_n \cong \exp(-G_n/kT) , \tag{6}$$

where

$$G_n \cong 4\gamma\sqrt{n} \quad n\,\Delta\mu \tag{7}$$

is the extra free energy after the formation of a cluster of n atoms on a (001) surface. Here γ is the extra free energy of an atom at the edge of the cluster. Note that $4a\sqrt{n}$ is an approximation to the edge length of a cluster of n atoms, where a is the lattice constant of the layer.

The rate of formation of 2-D nuclei at a site is [19]

$$J = Z\Gamma_{n^*} p_{n^*} . \tag{8}$$

Here n^* represents the number of atoms in a critical cluster, and it is the value of n which yields the maximum G_n in eq. (7). Γ_{n^*} is the rate of addition of atoms to a critical cluster, and Z is the Zeldovich non-equilibrium factor which accounts for a reduction in the number of clusters during steady-state nucleation.

We use $Z \cong (kT/16G_{n^*})^{1/2}\,\Delta\mu$ (see e.g. ref. [20], eq. (21b)), $\Gamma_{n^*} = 4\sqrt{n^*}\,k^+$, and eq. (6) to obtain

$$J = k^+(\Delta\mu/kT)^{1/2}\exp[-4\gamma^2/(kT\,\Delta\mu)]\ . \tag{9}$$

The expression for Γ_{n^*} and eq. (9) apply when atoms are added by direct impingement at the edges of the cluster. Surface migration effects are considered later. The exponential in eq. (9) is very small for values of $\Delta\mu$ in the range: $0 \leqslant \Delta\mu \leqslant \gamma^2/kT$, and this is therefore the range where screw dislocations are important. Clearly, the extent of this range is very sensitive to the edge free energy γ.

A step terminating on a screw dislocation tends to wind up into a spiral, whose shape and steady-state rotation rate have been calculated by Cabrera and Levine [18]. The found that the distance between adjacent arms of the spiral is $l \cong 19\ r^*$ where r^* is the radius of the critical nucleus. This result applies at large distances from the center. A dislocation with Burgers vector $b > 1$ produces b steps which terminate on the dislocation, and the rate of formation of new layers is

$$I = bc\,\Delta\mu/(19\,\gamma a)\ , \tag{10}$$

where c is the step velocity, and we use $r^* = (a/2)\sqrt{n^*}$. Two dislocations of opposite sign should produce new layers at approximately the same rate as an isolated dislocation if the distance separating them is greater than $2r^*$. Otherwise the rate is reduced because of the extra free energy required to expand the step segment joining them into a disk with the diameter of the critical nucleus.

Spiral growth combined with 2-D nucleation is somewhat difficult to treat analytically. The simpler case of 2-D nucleation has been solved by Kolmogoroff in the case of the growth of a monolayer on a flat substrate [21]. This solution can, however, be used to obtain an approximation to the steady-state crystal growth rate. In the following we apply the Kolmogoroff approach to steady-stage spiral growth with 2-D nucleation.

We consider a crystal surface with two different sources of disk-shaped nuclei. One, source A, produces nuclei at random positions at a rate $J\rho$ per unit area. This represents 2-D nucleation, and ρ is the number of sites per unit area. Source B produces nuclei at a rate I, but all of the nuclei originate from the same point P. This is a simplified model of the screw dislocation step source. At time $t = 0$ the two sources begin to generate nuclei on the flat surface and we calculate the probability $x(t)$ that point P is covered by a nucleus. The probability q_i that a nucleus formed during the time interval $(t_i,\ t_i + \Delta t_i)$ would cover P before time t $(t_i < t)$ is

$$q_i = \pi c^2(t - t_i)^2\,\rho J\,\Delta t_i + I\,\Delta t_i\ , \tag{11}$$

where Δt_i is sufficiently small that $q_i \ll 1$. The first term accounts for the probability that source A created a nucleus during Δt_i in the circle of radius $c(t - t_i)$, since only nuclei within this region would reach P before time t. Similarly, the second term is the probability that source B produced a nucleus during Δt_i, since any nucleus at P covers the point immediately. The probability of finding point P uncovered at time t is

$$1 - x(t) = \prod_i (1 - q_i)\ . \tag{12}$$

The product runs over all subintervals Δt_i in the interval $(0,\ t)$. We may use the approximation $1 - q_i \cong \exp(-q_i)$ and combine eqs. (11) and (12) to obtain

$$1 - x(t) = \exp\left[-\pi J\rho c^2 \int_0^t (t - t')^2\,\mathrm{d}t' - It\right]$$

$$= \exp(-\tfrac{1}{3}\pi J\rho c^2 t^3 - It)\ . \tag{13}$$

This model is not directly applicable to steady-state, multilayer growth since it restricts the growth process to a single layer; and the growth rate $\mathrm{d}x/\mathrm{d}t$ approaches zero as x approaches unity. However an estimate of the steady-state growth rate may be obtained if we approximate the time τ to grow one layer of the crystal in the steady state with the time required for $x(t)$ to reach some fraction of unity. We choose $x(\tau) = 1 - \mathrm{e}^{-1}$, since this yields the correct steady-state value $\tau^{-1} = I$ in the limit where $J = 0$. This choice of $x(\tau)$ and eq. (13) imply the general relation

$$\tfrac{1}{3}\pi J\rho c^2\tau^3 + I\tau = 1\ . \tag{14}$$

In the limit where $I = 0$, $\tau = (\tfrac{1}{3}\pi J\rho c^2)^{-1/3}$ and the rate of growth of the crystal surface is

$$R_{2\text{-D}} = d/\tau = d(\tfrac{1}{3}\pi J\rho c^2)^{1/3}\ , \tag{15}$$

where d is the layer spacing. Eq. (15) is identical with the expression derived by Hillig [22] for 2-D nucleation growth.

In general the cubic eq. (14) must be solved for τ. In the limit where one of the sources dominates, a simpler form is accurate. Defining $Q \equiv (\frac{1}{3}\pi J\rho c^2)^{1/3}$, we write eq. (14) as

$$(Q\tau)^3 + (I\tau) = 1 . \tag{16}$$

In the limit $I << Q$, (16) has the approximate solution

$$\tau^{-1} \cong Q + I/3 , \tag{17}$$

and for $I >> Q$,

$$\tau^{-1} \cong I[1 + (Q/I)^3] . \tag{18}$$

In neither of these limits is the combined rate of growth a simple sum of the rates Q and I derived for independent sources. According to (18), a relatively small rate J does not appreciably affect the growth rate when $I >> Q$.

The reason for this latter result can be understood from the following argument. In order for source A to have an effect on τ, an appreciable number of instances must occur in which source A produces a nucleus on top of the most recent nucleus formed by source B. If the nucleus of source A spreads and covers point P before B produces another nucleus, then source A has contributed to the growth at P. Only a very limited area is available for this process. The area of one nucleus at the instant source B produces the next one is $\pi c^2/I^2$. Hence the probability for source A to contribute a layer is $\sim J\pi c^2\tau/I^2 = 3(Q/I)^3$, in approximate agreement with eq. (18).

On the basis of this model, we now calculate the spiral growth regime, i.e., the values of temperature and driving force where the spiral growth mechanism has the predominant effect on the growth rate. As indicated in the previous discussion, 2-D nucleation is extremely slow at small values of $\Delta\mu$ and at low temperatures. We define, therefore, the spiral growth regime to be limited to those values of $\Delta\mu$ for which $Q \leqslant I/3$; here the inclusion of 2-D nucleation adds less than 4% to the growth rate according to eq. (18). This condition, together with eqs. (9), (10), and (15) yields the relation

$$\frac{\Delta\mu_0}{kT} = \frac{1.333\,(\gamma/kT)^2}{\ln\,[0.0168(c/k^+a)^{1/3}(\Delta\mu_0/kT)^{5/6}(kT/\gamma)b]} . \tag{19}$$

Here $\Delta\mu_0$ is the value of the chemical potential where $Q = I/3$, and we have replaced the density ρ of lattice sites by a^{-2}. This equation may be solved for $\Delta\mu_0$ by iteration, provided that we know the values for c and γ.

We approximate the velocity of the monatomic step with the expression

$$c = a(k^+ - k_3^-) = k^+a[1 - \exp(-\Delta\mu/kT)] . \tag{20}$$

This equation is equivalent to the Wilson–Frenkel law for crystal growth rates. It is based on the assumption that atoms in the edge of the step evaporate at the average rate k_3^-, which is the average evaporation rate under equilibrium conditions where $\Delta\mu = 0$ [2]. This is equivalent to assuming that the structure of the step is not affected by the impingement rate. Eq. (20) is a good approximation at high temperatures where the edge of the step is rough and contains a high density of kink sites even in equilibrium, but at low temperatures it overestimates the velocity. For the present purposes it is not necessary to have an accurate value of c since eq. (19) contains c in the argument of the logarithm with an exponent of one-third. On the other hand, the value of γ is critical, and we approximate this parameter by the interfacial free energy of the 2-D square lattice gas [23]

$$\gamma/kT = \varphi/2kT - \ln[\coth(\varphi/4kT)] . \tag{21}$$

Computer simulations [5] confirm our physical intuition that the edge of a step is accurately represented

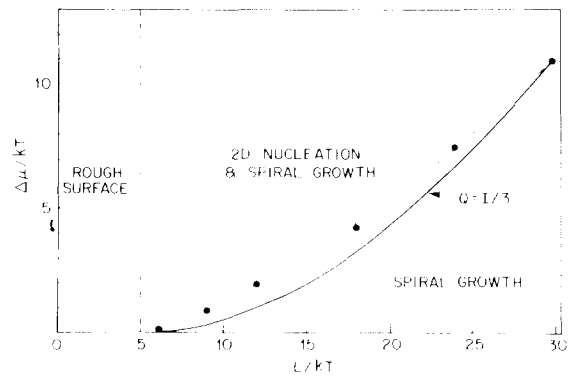

Fig. 3. The value of $\Delta\mu_0/kT$ in eq. (19), $b = 2$, is plotted as a function of L/kT (solid line). The solid circles indicate the values of $\Delta\mu$ where the Monte Carlo growth rate of a crystal surface containing dislocations with $b = 2$ is approximately three times that of a perfect crystal surface. The roughening transition occurs at $L/kT = 4.9$, indicated by the vertical dashed line.

by such a 2-D model, provided the temperature is less than about $0.8T_R$. The free energy γ in eq. (21) is zero at a critical temperature $T_c \cong 0.92T_R$, and in general eq. (21) underestimates the (010) step free energy.

Fig. 3 is a plot of $\Delta\mu_0/kT$ as a function of L/kT using eqs. (19), (20) and (21). An extensive screw dislocation regime is present at low temperature, but it vanishes as the temperature approaches T_R. The solid circles represent estimates of $\Delta\mu_0$ based on Monte-Carlo data. Apparently the large discrepancies near T_R result primarily from the approximations employed in the nucleation model. The clusters that appear at high temperatures are irregular in shape and seldom do we see the compact shapes assumed in classical nucleation theory. Also, interactions between subcritical clusters are not included in the theory, although they occur frequently at high temperatures. At the lower temperatures the theory and Monte-Carlo data are in good agreement [24].

4. Monte-Carlo calculations of growth rates

The Monte-Carlo simulations permit us to make a direct comparison of the growth rates of perfect crystals with those containing dislocations. First we consider growth in the absence of surface diffusion since most of our conclusions are apparent in these results. Later we examine the effect of surface diffusion on the growth rates.

The formation of a growth spiral is illustrated in fig. 4. The computer-generated drawings display an 80 X 80 section of a crystal, and a single dislocation with a Burgers vector of $b = 2$ terminates at the center [25]. Two

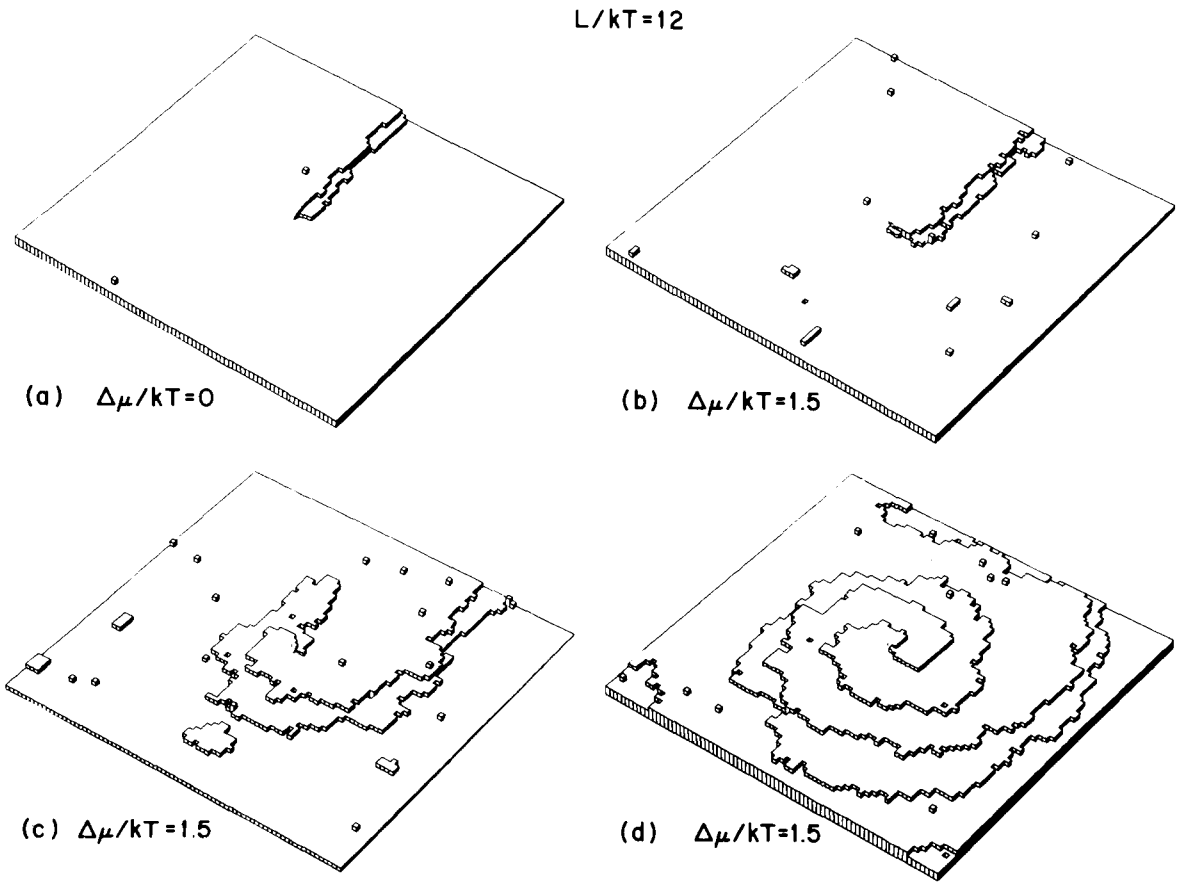

Fig. 4. Computer drawings of Monte Carlo microstates generated during the formation of a double spiral. Part (a) shows the steps in equilibrium, and (b)–(d) show successive stages as the steps wind up into a spiral with $\Delta\mu = 1.5kT$.

steps originate at the dislocation. A typical equilibrium configuration at $L/kT = 12$ appears in fig. 4a. Some quantitative observations may be noted directly in the figures, for example, the average number of kinks per unit length of the step is approximately [10]

$$\rho_k \cong 2a^{-1} \exp(-\varphi/2kT) , \qquad (22)$$

provided the system is in equilibrium. The segments of the two steps illustrated are $40a$ long and, according to (22), an ensemble average should yield ~10.8 kinks in each segment. Allowing for statistical fluctuations, this number is in good agreement with seven and ten kinks observed in the two segments shown.

Note that the two steps have separated from one another along most of their length. The fact that the steps cannot overlap one another produces a kind of repulsion between them, the random fluctuations in the position of each step causes the upper one to move to the left and the lower one to move to the right. This effect was termed a "kinetic repulsion" by Gruber and Mullins [26].

The approximate number of adatoms per unit area of the surface may be calculated from the ratio of the impingement rate to the evaporation rate,

$$\rho_1 = a^{-2}k^+/k_1^- = a^{-2} \exp(\Delta\mu/kT - 2\varphi/kT) . \qquad (23)$$

This expression applies when most of the impinging atoms form only one bond to the crystal, as is certainly the case in fig. 4a. In equilibrium the average number predicted by (23) for an 80 × 80 surface is 2.15, and two adatoms are observed in the figure.

The successive stages of growth as the steps wind up into a double spiral are shown in figs. 4b–4d. The steps tend to separate during growth, and again this is a result of the inability of a step to move in front of a lower one at any point. Using eqs. (7) and (21) we calculate the size of the critical nucleus to be $n^* = 5.3$ atoms. The surface in fig. 4b contains several clusters just below this size, and in fig. 4c several clusters larger than the critical size are observed. Reference to fig. 3 shows that $L/kT = 12$ and $\Delta\mu/kT = 1.5$ is in the spiral growth regime, but close to the borderline.

The difference in the impingement rate between figs. 4a and 4b–4d is directly reflected in the adatom population. Eq. (23) is applicable also to a crystal surface which is growing [27], and it applies most accurately to fig. 4b where the number of edge sites is small. According to (23) an average of 9.6 adatoms is expected, whereas six are observed. The steps in figs. 4b–4d contain a higher density of kink sites and two-bonded atoms than those of fig. 4a, and this is a result of the higher rate of random deposition in the edges of the steps.

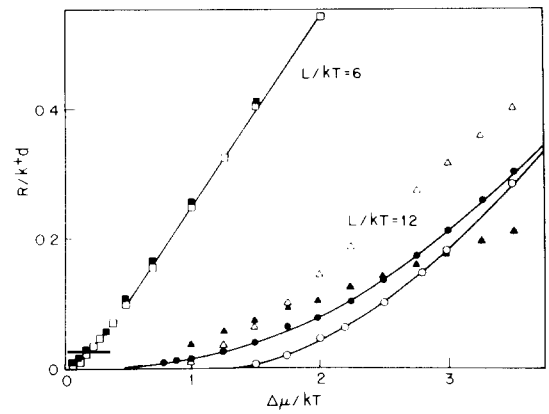

Fig. 5. Growth rates plotted versus $\Delta\mu/kT$ on a perfect crystal surface, and compared with the spiral growth rate (open and closed symbols, respectively). The squares represent the data taken as $L/kT = 6$; and the circles $L/kT = 12$. The triangles indicate analytical results for $L/kT = 12$.

The Monte-Carlo growth rates are plotted versus $\Delta\mu$ in fig. 5. At $L/kT = 6$ the growth rates of the crystal with the dislocations are practically indistinguishable from the perfect crystal growth rates. A Burgers vector of four is used to enhance the difference between the two rates. Very precise data near the origin would reveal significant differences, since there is a small nucleation barrier to the growth of the perfect crystal. Above T_R, however, dislocations apparently have little effect on the growth rate at any value of $\Delta\mu$.

At temperatures less than half T_R, i.e., the $L/kT = 12$ data, the screw dislocations cause an appreciable increase in the growth rate over that of the perfect crystal. The open circles are the Monte-Carlo growth rates of a perfect crystal, as in fig. 2. The closed circles correspond to the growth rates of a crystal containing screw dislocations with $b = 2$. The curves indicate the trends in the Monte-Carlo data. Dislocations are necessary for measurable growth at values of $\Delta\mu < kT$, but they have little effect for large $\Delta\mu$.

Some growth rates predicted by the analytical models of section 3 at $L/kT = 12$ are represented by the tri-

angles in fig. 5. The growth rate resulting from the spiral mechanism alone is

$$\frac{R}{k^+ d} = \frac{0.053 b \Delta\mu [1 - \exp(-\Delta\mu/kT)]}{\varphi/2kT - \ln[\coth(\varphi/4kT)]}, \qquad (24)$$

according to eqs. (10), (20), and (21). The closed triangles represent eq. (24), and they are somewhat above the corresponding Monte-Carlo data at small values of $\Delta\mu/kT$. The discrepancy is caused primarily by the use of the Wilson–Frenkel growth rate for the step velocity in eq. (20), the actual step velocity is much less. At the larger values of $\Delta\mu/kT$ the closed triangles fall below the closed circles because 2-D nucleation is included only in the Monte-Carlo data. The growth rate of a perfect crystal is according to eqs. (9), (15), and (20),

$$\frac{R}{dk^+} = \left(\frac{\pi}{3}\right)^{1/3} \left(\frac{\Delta\mu}{kT}\right)^{1/6} \left[1 - \exp\left(\frac{-\Delta\mu}{kT}\right)\right]^{2/3}$$

$$\times \exp\left(\frac{-4\gamma^2}{3kT\Delta\mu}\right). \qquad (25)$$

The open triangles correspond to this expression, where γ is obtained from eq. (21). Again eq. (25) predicts growth rates larger than the Monte-Carlo data, as a result of the high step velocity in eq. (20) and the high nucleation rate of eq. (9).

We now compare the Monte Carlo data with eq. (16), the relation between the total growth rate and the spiral and 2-D nucleation growth rates. Data on the perfect surface rate provide us with values for Q, and the data on the screw dislocation rate provide τ. Hence we need only to obtain I, the rate of formation of new layers in the absence of 2-D nucleation. This is accomplished by inhibiting the deposition of atoms on sites where they would have only one bond to the crystal. It is also essential to suppress the annihilation of one-bonded atoms, since the transition probabilities must satisfy the condition

$$k_1^- = k_1^+ \exp[(2\varphi - \Delta\mu)/kT], \qquad (26)$$

in order to obey microscopic reversibility at equilibrium. We observe that one-bonded atoms are generally present even during growth, since they are formed by the evaporation of the lateral neighbor of a two-bonded atom.

The growth rate of the crystal containing screw dislocations and with $k_1^+ = 0$ is plotted in fig. 6, together with the data from fig. 5. The dotted line is the growth

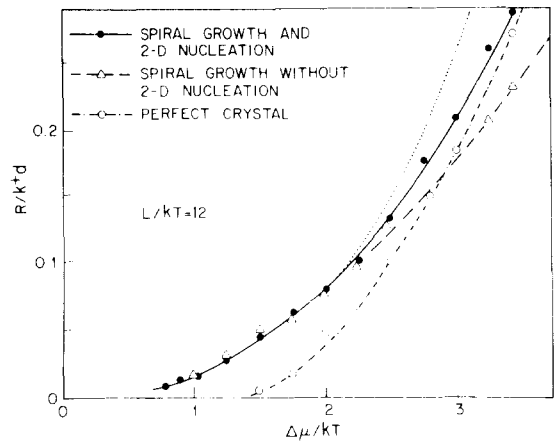

Fig. 6. Plot of the $L/kT = 12$ Monte-Carlo growth rates as in fig. 5, but with the addition of the spiral growth data in the absence of 2-D nucleation (open triangles). The dotted line is a plot of the growth rate calculated by eq. (16).

rate $d\tau^{-1}$ predicted by eq. (16), where I and Q are obtained from the broken and dot-dashed curves, respectively. Eq. (16) yields a somewhat larger combined growth rate than that which was measured at the higher values of $\Delta\mu$. Under these conditions $I \ll Q$, and during steady-state growth the screw dislocation steps merge very quickly with those arising from 2-D nucleation. During the early stages of growth, the monolayer model of eq. (16) must have a very smooth surface reflecting the initial configuration. The probably accentuates the effect of source B on the growth rate since a large number of nuclei is always present in the actual system. The empirical relation $\tau^{-1} = (Q^3 + I^3)^{1/3}$ was suggested by Bertocci [6]. This expression affords a better fit to the data, but it too overestimates the growth rate.

The structure of the growth spiral is a function of the temperature and the deposition rate. Fig. 7 illustrates spirals which formed at $\Delta\mu = 3kT$, and at various temperatures. At the lowest temperature, $L/kT = 30$, the step edges are straight and oriented along the close-packed ⟨100⟩ directions. Under these conditions, the motion of a step segment is largely determined by the rate of one-dimensional nucleation in the edge of the step [28]. A pair of atoms in adjacent positions along the edge is a supercritical nucleus, and once such a pair forms, it can elongate rapidly by the addition of atoms to the kink sites at both ends. The nucleation rate is proportional to the number of single edge atoms which can be promoted to pairs by the random impingement

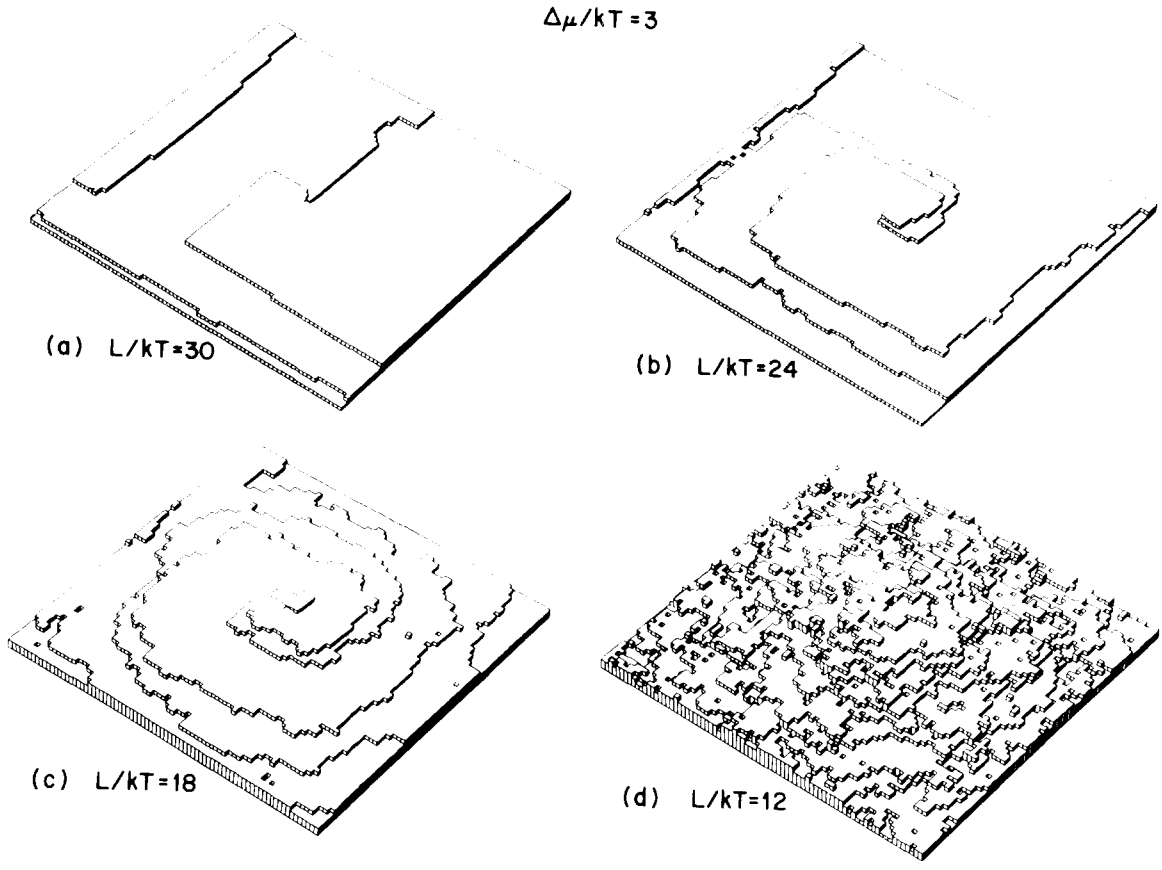

Fig. 7. Non-equilibrium surfaces of crystals containing a single screw dislocation, $b = 2$, at various temperatures. Here $\Delta\mu = 3kT$.

process. The average velocity of the step increases with the length of the step segment because the number of edge atoms is roughly proportional to the length. For this reason, the separation between adjacent arms of the spiral increases with the distance from the center, as seen in figs. 7a and 7b. At the higher temperatures thermal fluctuations produce a number of kink sites even in the short segments, and the step velocity is essentially independent of its length. The separation between adjacent arms of the spiral according to the Cabrera–Levine formulation is [18]

$$l = 19(\gamma/kT)a/(b\,\Delta\mu/kT)\,. \tag{27}$$

Decreasing L/kT causes a corresponding reduction in γ/kT according to eq. (21), and hence l becomes smaller. This is readily apparent in spirals of fig. 7, and at $L/kT = 12$ the spiral arms are so closely spaced that it is difficult to distinguish them.

A high deposition rate also produces a spiral with closely spaced arms, according to eq. (27). Comparison of fig. 4d with fig. 7c shows the dramatic change caused by doubling the value of $\Delta\mu$. The structure of the spiral formed at $L/kT = 12$ and $\Delta\mu/kT = 1.5$ is very similar to the one in fig. 7c where $L/kT = 18$ and $\Delta\mu/kT = 3$. This is in approximate agreement with eq. (27), since the ratio $\gamma/\Delta\mu$ is similar in these two cases.

Surface migration occurs in most vapor growth systems, since it generally requires less energy to translate an atom parallel to the surface than to remove it altogether. We examine the case summarized by eqs. (3), (4) and (5) where an adatom may hop to a neighboring site with a frequency $k_{11} = \nu \exp(-\varphi/2kT)$, which is larger than the frequency of evaporation, $k_1^- = \nu \exp(-\varphi/kT)$. The adatom generally hops to a number of surface sites before it evaporates. It is the opportunity for joining a kink site in a step edge or adatom clus-

ter which causes an enhancement in the growth rate.

The flux to an isolated step can be calculated analytically. We assume for simplicity that the step is perfectly straight, infinitely long, and parallel to a ⟨100⟩ direction. We again assume that the average evaporation rate is k_3^- per edge atom. Then, as in the model employed for the derivation of eq. (20), the flux of atoms per site at the edge of the step resulting from direct impingement and evaporation is

$$J_0 = k^+ - k_3^- . \tag{28}$$

In addition, we must include the flux resulting from the migration of atoms to and from the edge of the step.

The probabilities n_j of finding adatoms on sites j units from the edge of the step are related by the set of conservation equations

$$\mathrm{d}n_j/\mathrm{d}t = k^+ + \tfrac{3}{8}k_{11}(n_{j+1} + n_{j-1}) - \tfrac{3}{4}k_{11}n_j - k_1^- n_j . \tag{29}$$

The first term on the right corresponds to addition by direct impingement on the site, the second accounts for a migration to the site of an atom in an adjacent row. The factor $\frac{3}{8}$ appears since only three of the eight possible migration jumps would move an atom from row $j+1$ to row j, for example. The third term accounts for migration from the site, and the factor $\frac{3}{4}$ is required since only six of the eight jumps remove an atom from row j. Finally, $k_1^- n_j$ is the evaporation rate from the site. Note that we neglect any clustering of adatoms in this formulation.

In the steady state, $\mathrm{d}n_j/\mathrm{d}t = 0$, eq. (29) is satisfied by an expression of the form

$$n_j = (k^+/k_1^-)(1 - A\,\mathrm{e}^{-\lambda j}) , \tag{30}$$

where A and λ are constants to be determined by the equations. Substitution of eq. (30) into (29), yields

$$\lambda = 2\ln[(\tfrac{2}{3}k_1^-/k_{11})^{1/2} + (\tfrac{2}{3}k_1^-/k_{11} + 1)^{1/2}] . \tag{31}$$

The concentration n_1 at a site one unit removed from the edge of the step obeys the relation

$$\mathrm{d}n_1/\mathrm{d}t = k^+ + \tfrac{3}{8}k_{11}(n_2 + k_3^-/k_1^-) - \tfrac{3}{4}k_{11}n_1 - k_1^- n_1 . \tag{32}$$

This equation is identical with eq. (29) with $j = 1$, except for the replacement of n_0 in (29) by k_3^-/k_1^-, the equilibrium density of adatoms. This is consistent with the previous assumption that the average evaporation rate from the sites at the edge of the step is the equilibrium rate. Substitution of eq. (30) into the steady-state form of (32) yields

$$A = (1 - k_3^-/k^+)/[2\,\mathrm{e}^{-\lambda} + \tfrac{8}{3}(k_1^-/k_{11})\,\mathrm{e}^{-\lambda} - \mathrm{e}^{-2\lambda}] . \tag{33}$$

The surface flux to the step results from the exchange between the atoms in the edge of the step and the adatoms in the adjacent row of sites, that is

$$J_s = \tfrac{3}{8}k_{11}(n_1 - n_0) = \tfrac{3}{8}(k_{11}/k_1^-)[(k^+ - k_3^-) - k^+ A\,\mathrm{e}^{-\lambda}] , \tag{34}$$

where n_1 is eliminated in the expression on the right by the use of eq. (30). Eqs. (31) and (33) provide the needed expressions for A and λ, and after some manipulation we achieve the simple result

$$J_s = (k^+ - k_3^-)[(\tfrac{1}{4} + \tfrac{3}{8}k_{11}/k_1)^{1/2} - \tfrac{1}{2}] . \tag{35}$$

The velocity of the step as a result of direct impingement and migration of adatoms on both sides is

$$c = a(J_0 + 2J_s) = ak^+[1 - \exp(-\Delta\mu/kT)](1 + \tfrac{3}{2}k_{11}/k_1)^{1/2} . \tag{36}$$

Fig. 8 is a plot of screw dislocation and perfect

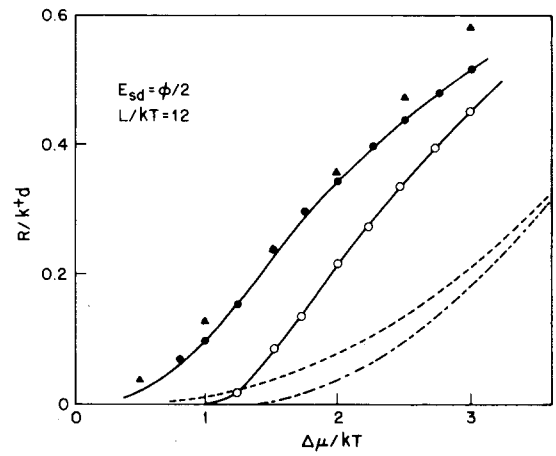

Fig. 8. Spiral and perfect crystal growth rates (closed and open circles) caluclated with the surface migration probabilities of eqs. (3)–(5). The triangles represent the spiral growth rate calculated with eqs. (10), (21) and (36). The dashed curves indicate the growth rates calculated without surface migration.

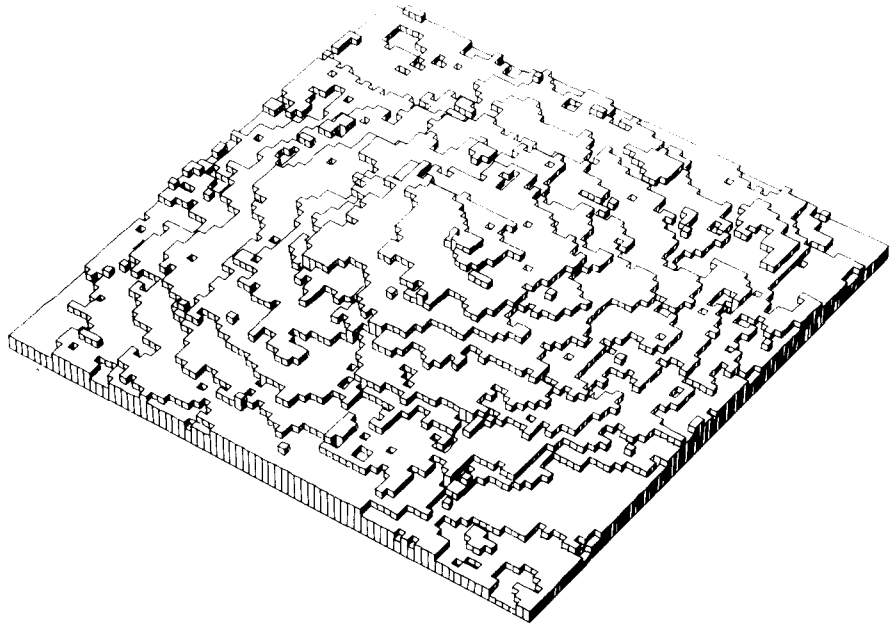

Fig. 9. Non-equilibrium surface of a crystal containing a screw dislocation, $h = 2$, with surface migrations included. Here $L/kT = 12$, $\Delta\mu/kT = 3$.

crystal growth rates, both calculated in the presence of surface migration. The dashed curves indicate the growth rates calculated without surface migration. The ratio of the migration to evaporation rate is $k_{11}/k_1 = 7.4$ at the indicated temperature. The spiral growth rate derived from eq. (36) together with (10) and (21) is indicated by the triangles. The competition between adjacent arms of the spiral for the surface migration flux was neglected in the derivation of (36), and this is an important factor at larger values of $\Delta\mu$ where the arms are closely spaced. The agreement between theory and the Monte-Carlo data at small $\Delta\mu$ values contrasts with the earlier observation, in the absence of surface diffusion, that the theoretical growth rates were about a factor of two larger than those calculated by the Monte-Carlo method. The reason for the better agreement is related to the evaporation rate for atoms at the edge of the step. The actual evaporation rate during growth is generally higher than the equilibrium rate since the larger impingement rate causes some extra roughening of the step edges. Migration along the edge of the step tends to reduce this effect, since an atom adsorbed along the edge may migrate to a kink site. In this case there is sufficient mobility of the atoms in the edge to maintain an evaporation rate close to the equilibrium value [29]. According to the Monte-Carlo data, the addition of surface diffusion causes about a sixfold increase in the growth rate at low values of $\Delta\mu$. The increase which results from adatom diffusion is ~3.5 according to eqs. (20) and (36). The reduction in the evaporation rate in the step edges must account for the remaining increase. Gilmer and Bennema [15] simulated the growth of stepped surfaces at $L/kT = 6$ with surface migration, and in this case adatom diffusion alone accounts for the increase in the growth rate. The high density of kink sites at this temperature apparently accommodates the increased impingement rate, even in the absence of surface migration.

A growth spiral formed at $L/kT = 12$ and $\Delta\mu/kT = 3$ is shown in fig. 9. Comparison with fig. 7d does reveal a somewhat smoother edge structure, in particular, the number of two-bonded atoms is appreciably smaller.

5. Conclusions

The spiral growth mechanism has a significant effect on kinetics in a limited range of low temperatures and small driving forces. Screw dislocations do not affect

the kinetics, for example, of crystals that are grown from the melt and have a small entropy of fusion. In this case even the close-packed faces are apparently quite rough on an atomic scale, and screw dislocation ledge sources are superfluous. In another system, the sticking coefficients measured for vapor deposition on low temperature substrates may not be substantially affected by the presence of screw dislocations. In this case, the large driving forces which are generally present permit rapid 2-D nucleation, and again the screw dislocation ledge source is not needed. However, in each case the relative importance of spiral growth must be considered on the basis of the experimental values of the driving force and temperature, and of the binding energy of the lattice. In fact, fig. 3 may be used semi-quantitatively by comparing the α-factor of the crystallographic face in question with that of the simple cubic (001) face considered here.

Surface mobility causes a large increase in the growth rate. Not only does it increase the flux of atoms to the edge of a step, but it also reduces the evaporation rate from the step. The extent of the spiral growth regime is not affected significantly by surface mobility since the growth rates of perfect crystals and of those containing screw dislocations are increased by approximately the same factor.

Acknowledgments

The author is indebted to H.J. Leamy, K.A. Jackson and J.D. Weeks for many helpful discussions.

References

[1] H.J. Leamy and K.A. Jackson, J. Appl. Phys. 42 (1971) 2121.
[2] G.H. Gilmer and P. Bennema, J. Appl. Phys. 43 (1972) 1347.
[3] R.A. Hunt and B. Gale, J. Phys. C6 (1973) 3571.
[4] G.H. Gilmer, K.A. Jackson, H.J. Leamy and J.D. Weeks, J. Phys. C7 (1974) L123.
[5] H.J. Leamy and G.H. Gilmer, J. Crystal Growth 24/25 (1974) 499.
[6] U. Bertocci, Surface Sci. 15 (1969) 286.
[7] C. van Leeuwen and F.H. Mischgofsky, J. Appl. Phys. 46 (1975) 1056.
[8] F.F. Abraham and G.H. White, J. Appl. Phys. 41 (1970) 1841.
[9] F.C. Frank, Discussions Faraday Soc. No. 5 (1949) 48.
[10] W.K. Burton, N. Cabrera and F.C. Frank, Phil. Trans. Roy. Soc. London 243A (1951) 299.
[11] H.J. Leamy, G.H. Gilmer and K.A. Jackson, in: Surface Physics of Materials, I, Ed. J.M. Blakely (Academic Press, New York, 1975) p. 121.
[12] K.A. Jackson, in: Liquid Metals and Solidification (Am. Soc. Metals, Metals Park, Ohio, 1958) p. 174.
[13] K.A. Jackson, in: Crystal Growth, Ed. H.S. Peiser (Pergamon, Oxford, 1967) p. 17.
[14] R.L. Schwoebel, J. Appl. Phys. 40 (1969) 614.
[15] P. Bennema and G.H. Gilmer, in: Crystal Growth: An Introduction, Ed. P. Hartman (North-Holland, Amsterdam, 1973) p. 263.
[16] C.S. Kohli and M.B. Ives, J. Crystal Growth 16 (1972) 123.
[17] Figs. 4 and 7 are, however, constructed as though the lattice were displaced. This eliminates the unphysical step which would otherwise appear along the line AD, and it simplifies the interpretation since the interactions across the plane ABCD are not displaced.
[18] N. Cabrera and M.M. Levine, Phil. Mag. 1 (1956) 450.
[19] K.C. Russell, in: Phase Transformations (Am. Soc. for Metals, Metal Park, Ohio, 1970).
[20] B. Lewis, J. Crystal Growth 21 (1974) 29.
[21] A.N. Kolmogorov, Izv. Akad. Nauk Ser. Math. No. 3 (1937) 355.
[22] W.B. Hillig, Acta Met. 14 (1966) 1968.
[23] L. Onsager, Phys. Rev. 65 (1944) 117.
[24] The accuracy of the nucleation equation is also limited at high deposition rates and very low temperatures. Eq. (9) is derived by replacing a sum over discrete clusters (containing $n = 1, 2, \ldots$ atoms) by an integral. But at $L/kT = 30$ and $\Delta\mu/kT = 11$, for example, eq. (7) implies that $n^* = 0.8$, and the integral should not be expected to provide an accurate approximation of the sum. Also, the Cabrera–Levine expression in eq. (10) involves similar assumptions. As it happens, the integral is an accurate approximation of the sum even at $L/kT = 30$ and $\Delta\mu/kT = 11$, but at higher driving forces large discrepancies occur.
[25] The drawings of figs. 4 and 7 display only half of the crystal surface. The simulated crystal contains another dislocation, the mirror image of the one displayed, and both steps terminate on this dislocation. The $(00\bar{1})$ face contains 80×160 sites.
[26] E.E. Gruber and W.W. Mullins, J. Phys. Chem. Solids 28 (1967) 875.
[27] Eq. (23) is derived by equating the rates of condensation and evaporation of adatoms, i.e., $\rho_1 k_1^- = k^+$. Two assumptions are implied here: first, it is assumed that condensation on any site on the crystal surface produces an adatom, and second, there is no net production or absorption of adatoms due to other processes than condensation and evaporation. The second condition is not strictly satisfied during growth of the crystal since some adatoms are absorbed by the moving steps. But since the rate of absorption of adatoms in step edges is generally very low

in comparison to the rate at which condensation–evaporation equilibrium is established ($\sim k\bar{1}$), eq. (23) can be applied to crystal surfaces which are growing.

[28] J.C. Angus and T.J. Dyble, Surface Sci. 50 (1975) 157.

[29] An atom adsorbed in the edge of a straight step makes an average of approximately one jump along the edge. Then it either hops to the adjacent terrace or evaporates. (See eqs. (4) and (5) for the actual probabilities.) Since the equilibrium kink spacing is $\sim 3.6a$ in this case, it seems inconsistent that the edge evaporation rate should approach the equilibrium value. However, an analysis of the coupled edge and surface diffusion equations governing migration to the kinks is required. Such a study reveals that the edge concentration may approach the equilibrium value, even when the kink spacing is much greater than the edge migration distance (R. Ghez, private communication). This occurs when the surface migration distance is large and the atom that migrates from the edge to the terrace has a high probability of migrating back to the edge before evaporating.